Infrared Identification of Matrix Isolated H 2 O·O 2

ARTICLE *in* THE JOURNAL OF PHYSICAL CHEMISTRY A · JUNE 2005

Impact Factor: 2.69 · DOI: 10.1021/jp050040v · Source: PubMed

Infrared Identification of Matrix Isolated $H_2O \cdot O_2$

Paul D. Cooper,[†] Henrik G. Kjaergaard,[‡] Vaughan S. Langford,[§] Allan J. McKinley,[†] Terence I. Quickenden,*[,†] Timothy W. Robinson,[‡] and Daniel P. Schofield[‡]

Chemistry M313, School of Biomedical and Chemical Sciences, The University of Western Australia, 35 Stirling Highway, Crawley, WA 6009, Australia, Department of Chemistry, University of Otago, P.O. Box 56, Dunedin, New Zealand, and Department of Chemistry, University of Canterbury, Private Bag 4800, Christchurch New Zealand

Received: January 4, 2005; In Final Form: March 19, 2005

Theoretical studies of the $H_2O \cdot O_2$ complex have been carried out over the past decade, but the complex has not previously been experimentally identified. We have assigned IR vibrations from an $H_2O \cdot O_2$ complex in an inert rare gas matrix. This identification is based upon theoretical calculations and concentration dependent behavior of absorption bands observed upon codeposition of H_2O and O_2 in argon matrixes at 11.5 ± 0.5 K. To aid assignment, we have used a harmonically coupled anharmonic oscillator local mode model with an ab initio calculated dipole moment function to calculate the OH-stretching and HOH-bending frequencies and intensities in the complex. The high abundance of H_2O and O_2 makes the $H_2O \cdot O_2$ complex likely to be significant in atmospheric and astrophysical chemistry.

Introduction

The existence of an $H_2O \cdot O_2$ complex was first proposed nearly 50 years ago. Heidt and co-workers[1,2] observed an increase in the UV absorption of liquid water when oxygen gas was dissolved in solution. No physical explanation for this phenomenon was available at the time, but it was proposed that complexes of $H_2O \cdot (O_2)_x$ were responsible for this increase of absorption. Some 40 years later, there was a renewed[3−5] interest in the $H_2O \cdot O_2$ complex when it was suggested the complex was involved in the photonucleation of pure water vapor via UV absorption of $H_2O \cdot O_2$ to form a $H_2O^+ \cdot O_2^-$ charge-transfer (CT) complex. The large dipole moment of the CT complex subsequently attracts other water molecules, and clusters are formed. Cacace et al.[6] subsequently provided experimental evidence for the CT complex. It was found that the complex is metastable with a lifetime exceeding 0.5 μs, supporting the photonucleation theory. This suggests that it is important not only in the chemistry of water clusters but also in aerosol formation in the atmosphere.

There has been no observation of ground state $H_2O \cdot O_2$ using infrared spectroscopy. In the absence of experimental data, there have been numerous theoretical treatments[7−12] providing calculated physical properties such as geometry, binding energy, and electronic states as well as predicting electronic and infrared transitions. These calculations show that the complex is very weak, with a calculated binding energy of 0.72 kcal/mol, in comparison to 5.1 kcal/mol for the $H_2O \cdot H_2O$ complex.[11] A recent conference paper[13] has given assignments of rotational transitions of $H_2O \cdot O_2$ using the supersonic jet technique and Fourier transform microwave spectroscopy.

It is known that condensed phase reactions occurring in the Earth's atmosphere play a role in atmospheric phenomena, for example, in the formation of the Antarctic ozone hole.[14] Weakly bound complexes, considered as precursors to the condensed phase, are important because perturbations and interactions between the monomer units can alter the spectroscopy and reactivity compared with the constituent molecules.[15,16] Water is also a major component in the absorption of radiation in the atmosphere and is a key component in the Earth's radiative balance. The high abundances of H_2O and O_2 in the atmosphere may result in levels of $H_2O \cdot O_2$ that could affect the Earth's climate.[15,17,18]

Molecular oxygen has been spectroscopically observed in the surface of the Jovian satellites, Ganymede[19] and Europa.[20] The shape of the observed absorption bands is similar to those of solid β-O_2[21] with discrepancies thought to be caused by perturbations from other molecules.[22] The surfaces of Ganymede and Europa are covered in water ice, so it is likely that there are interactions between water molecules and oxygen molecules. Such interactions may alter the chemistry and spectral features of the icy surfaces of these and other satellites, and interstellar grains. Although the matrix isolation experiments presented here do not directly simulate the icy surfaces on outer solar system bodies, they do provide valuable information about similar species contained in inert gas matrixes where spectroscopic identification is more reliable.

In addition to the possible physical significances of $H_2O \cdot O_2$ complexes, there is fundamental knowledge to be gained about the nature of hydrogen bonding. The past decade has seen an extensive array of theoretical and experimental investigations into hydrated complexes of species, particularly those of atmospheric interest. Species similar to $H_2O \cdot O_2$, such as $H_2O \cdot N_2$,[23] $H_2O \cdot HO$,[24−26] $H_2O \cdot O_3$,[27] $H_2O \cdot O_2^+$,[28] $H_2O \cdot HO_2$[29], and $H_2O \cdot H_2O$,[30] have been identified via infrared matrix isolation spectroscopy due to spectral shifts in the vibrational frequencies caused by complexation. We present here the first infrared experimental evidence for the existence of the $H_2O \cdot O_2$ complex.

Computational Details

The dimensionless oscillator strength, *f*, of the transition from the vibrational ground state, g, to an excited state, e, is given

* Corresponding author. E-mail: tiq@chem.uwa.edu.au.
[†] The University of Western Australia.
[‡] University of Otago.
[§] University of Canterbury.

10.1021/jp050040v CCC: $30.25
Published on Web 04/21/2005

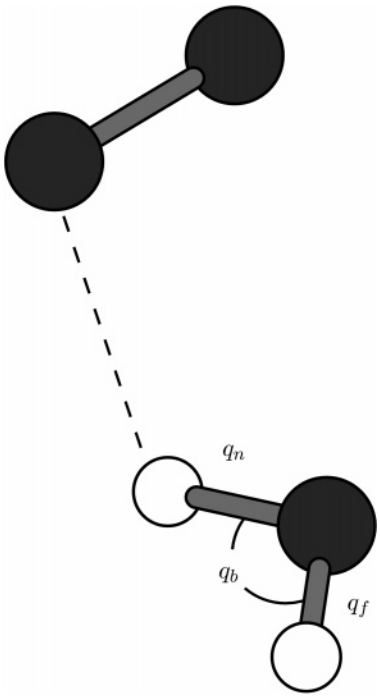

Figure 1. QCISD/6-311++G(2d,2p) optimized structure of the $H_2O{\cdot}O_2$ complex from refs 11 and 12.

by[31]

$$f = 4.702 \times 10^{-7}[\text{cm D}^{-2}]\tilde{\nu}_{\text{eg}}|\vec{\mu}_{\text{eg}}|^2 \quad (1)$$

where $\tilde{\nu}_{\text{eg}}$ is the vibrational wavenumber of the transition (in inverted centimeters) and $\vec{\mu}_{\text{eg}} = \langle \text{e}|\vec{\mu}|\text{g}\rangle$ is the transition dipole matrix element (in Debyes).

Previously, the OH-stretching spectrum of $H_2O{\cdot}O_2$ was calculated with a harmonically coupled anharmonic oscillator (HCAO) local mode model that included the OH-stretching vibrations.[11] Here, we describe both the OH-stretching and HOH-bending vibrations in the water unit of $H_2O{\cdot}O_2$ with the HCAO local mode model. The OH-stretching and HOH-bending modes are described as Morse oscillators. The zeroth-order Hamiltonian can be written as[32,33]

$$(H - E_{|0\rangle|0\rangle|0\rangle})/hc = \upsilon_{\text{n}}\tilde{\omega}_{\text{n}} + \upsilon_{\text{f}}\tilde{\omega}_{\text{f}} + \upsilon_{\text{b}}\tilde{\omega}_{\text{b}} - (\upsilon_{\text{n}}^2 + \upsilon_{\text{n}})\tilde{\omega}_{\text{n}}x_{\text{n}} - (\upsilon_{\text{f}}^2 + \upsilon_{\text{f}})\tilde{\omega}_{\text{f}}x_{\text{f}} - (\upsilon_{\text{b}}^2 + \upsilon_{\text{b}})\tilde{\omega}_{\text{b}}x_{\text{b}} \quad (2)$$

where $E_{|0\rangle|0\rangle|0\rangle}$ is the energy of the vibrational ground state, υ_i are the vibrational quantum numbers of the three oscillators, and $\tilde{\omega}_i$ and $\tilde{\omega}_i x_i$ are the local mode frequencies and anharmonicities of oscillators. The structure of $H_2O{\cdot}O_2$ is shown in Figure 1 with the three internal coordinates labeled. The labels b, n, and f stand for the HOH-bending, near OH-stretching, and far OH-stretching coordinates, respectively. The coupling between the three oscillators is described by the perturbation

$$H'/hc = -\gamma'(a_{\text{n}}^{+}a_{\text{f}} + a_{\text{n}}a_{\text{f}}^{+}) + fr'_{\text{nb}}(a_{\text{n}}^{+}a_{\text{b}}a_{\text{b}} + a_{\text{n}}a_{\text{b}}^{+}a_{\text{b}}^{+}) + fr'_{\text{fb}}(a_{\text{f}}^{+}a_{\text{b}}a_{\text{b}} + a_{\text{f}}a_{\text{b}}^{+}a_{\text{b}}^{+}) \quad (3)$$

where a and a^+ are the step-up and step-down operators known from harmonic oscillators. The coupling parameter, γ', describes the stretch−stretch coupling, while fr'_{nb} and fr'_{fb} describe the Fermi resonance coupling between the bending mode and the OH_n- or OH_f-stretching mode, respectively. These coupling constants contain both kinetic and potential energy contributions.[32,34] All coupling parameters are determined from ab initio calculations. The local mode frequencies and anharmonicities are determined from ab initio calculated potential energy curves as detailed previously.[33,35,36]

For the water unit in $H_2O{\cdot}O_2$, the dipole moment function is approximated by a series expansion in the internal OH-stretching and HOH-bending displacement coordinates about the equilibrium geometry. For two stretching coordinates and one bending coordinate, we have[32]

$$\vec{\mu}(q_{\text{n}},q_{\text{f}},q_{\text{b}}) = \sum_{ijk}\vec{\mu}_{ijk}q_{\text{n}}^{i}q_{\text{f}}^{j}q_{\text{b}}^{k} \quad (4)$$

where the coefficients $\vec{\mu}_{ijk}$ are given by

$$\vec{\mu}_{ijk} = \frac{1}{i!j!k!}\frac{\partial^{i+j+k}\vec{\mu}}{\partial q_{\text{n}}^{i}\,\partial q_{\text{f}}^{j}\,\partial q_{\text{b}}^{k}} \quad (5)$$

The summation in eq 4 is limited to sixth-order diagonal terms and third-order off-diagonal terms, and only off-diagonal terms that involve two coordinates are included. The dipole moment coefficients are determined from ab initio calculated dipole moment surfaces as detailed previously.[33]

The frequency of the OO-stretching transition in the complex $\nu_4(H_2O{\cdot}O_2)$ is predicted by

$$\nu_4(H_2O{\cdot}O_2) = \nu_4(O_2) + \Delta\nu_4(\text{DH}) \quad (6)$$

where ν_4 (O_2) is the observed OO-stretching frequency in molecular oxygen[37] and $\Delta\nu_4$(DH) is the difference in calculated harmonic frequency between the complex and molecular oxygen using the double harmonic approximation as implemented in Gaussian 94.[38] The intensity of the OO-stretching transition in the complex is obtained from the double harmonic calculation.

The ab initio calculations were performed using the quadratic configuration interaction including singles and doubles (QCISD) method with the 6-311++G(2d,2p) basis set in Gaussian 94.[38] The dipole moments are calculated as the analytical derivatives of the energy.

Experimental Details

All experiments were performed using a rotatable closed cycle helium refrigerator (CTI-Cryogenics 8300 compressor and a 350CP displacer) with a backing pressure in the matrix isolation system of $\sim 10^{-7}$ Torr. Distilled water was degassed several times via the freeze−pump−thaw method before mixing it with high purity oxygen and argon via standard manometric techniques in $H_2O/O_2/Ar$ ratios of 1:0:3000 to 1:150:1000. The mixtures were stored in stainless steel reservoirs at pressures typically between 600 and 1000 Torr before being deposited onto a KBr sample window held at 11.5 ± 0.5 K at a rate of $\sim$5−8 mmol h^{-1}. A Lakeshore DT-7470 silicon diode sensor was used to measure the sample temperature. Infrared spectra of the matrixes were obtained at a 0.5 cm^{-1} resolution with a Mattson Sirius 100 FTIR spectrometer.

Results and Discussion

The optimized geometry of the $H_2O{\cdot}O_2$ complex is taken from our previous work and is shown in Figure 1.[11] This structure is in agreement with the recent calculations of Sabu et al.[39] The calculated peak positions and intensities in water and the $H_2O{\cdot}O_2$ complex are given in Table 1 using the local mode parameters in Table 2. The effect of complexation with O_2 on the water molecule is minimal, with changes in vibrational

TABLE 1: Calculated OH-Stretching, HOH-Bending, and OO-Stretching Band Positions and Intensities in the $H_2O{\cdot}O_2$ Complex

	H_2O		$H_2O{\cdot}O_2$	
mode	$\bar{\nu}$	f	$\bar{\nu}$	f
ν_4[a]			1551	2×10^{-7}
$\|0\rangle_n\|0\rangle_f\|1\rangle_b \equiv \nu_2$	1596	1.29×10^{-5}	1593	1.56×10^{-5}
$\|0\rangle_n\|0\rangle_f\|2\rangle_b \equiv 2\nu_2$	3148	1.99×10^{-8}	3142	1.82×10^{-9}
$\|1\rangle_n\|0\rangle_f\|0\rangle_b + \|0\rangle_n\|1\rangle_f\|0\rangle_b \equiv \nu_1$	3658	1.03×10^{-6}	3661	6.55×10^{-7}
$\|1\rangle_n\|0\rangle_f\|0\rangle_b - \|0\rangle_n\|1\rangle_f\|0\rangle_b \equiv \nu_3$	3755	8.96×10^{-6}	3753	1.08×10^{-5}

[a] The peak position and oscillator strength are obtained from the double harmonic calculation; see text.

TABLE 2: Calculated Local Mode Parameters in the $H_2O{\cdot}O_2$ Complex

	H_2O[a]	$H_2O{\cdot}O_2$
$\tilde{\omega}_f$	3869.6	3869.7
$\tilde{\omega}x_f$	82.06	81.76
$\tilde{\omega}_n$		3869.4
$\tilde{\omega}x_n$		81.98
$\tilde{\omega}_b$	1636.4	1634.2
$\tilde{\omega}x_b$	20.4	20.62
γ'	47.27	47.41
fr'_{fb}	17.41	17.07
fr'_{nb}		17.67

[a] $\tilde{\omega}$ and $\tilde{\omega}x$ for water from ref 31.

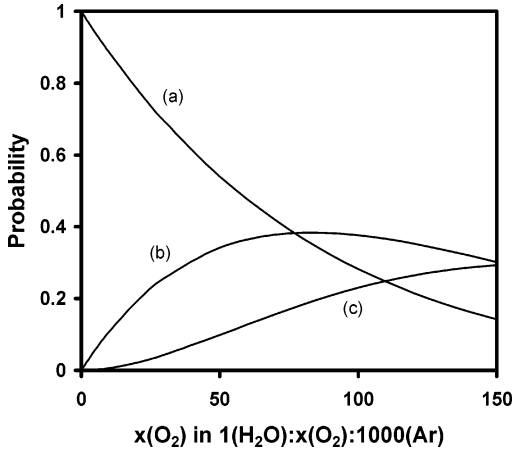

Figure 2. Probability distribution of a single H_2O molecule having (a) 0 O_2, (b) 1 O_2, and (c) 2 O_2 nearest neighbors in a hexagonal close packed argon lattice.

frequency in the order of a few wavenumbers. While our spectral resolution is sufficient to discern these shifts, there are several other experimental factors that complicate the assignment of vibrations to the complex. The matrixes that are formed in the experiments inevitably have relatively large amounts of H_2O monomer, with lesser, but significant, amounts of $H_2O{\cdot}H_2O$. Absorptions from these water species dominate the spectra. The amount of dimer can be reduced by decreasing the water concentration at the cost of decreasing the concentration of $H_2O{\cdot}O_2$. By making the water fraction in our matrixes much smaller than O_2, it also reduces the possibility of forming $(H_2O)_x{\cdot}O_2$ complexes that may complicate any assignments. The amount of complex formed in the matrix can be modeled by a probability distribution, as shown in Figure 2 for a 1:*X*:1000 $H_2O/O_2/Ar$ mixture ($X = 0-150$). This model assumes that the complex is formed by an H_2O molecule and an O_2 molecule being deposited adjacent to one another in a hexagonal close packed argon lattice and that no complex is formed in the gas stream prior to deposition. The model also assumes that H_2O and O_2 are deposited into the matrix by filling the position of an Ar atom in the lattice without any disruption to the crystal structure. The probability that a water molecule has *n* nearest neighbor O_2 molecules is given by

$$^{12}C_n(P_{oxy})^n(P_{Ar})^{12-n} \tag{7}$$

where P_{oxy} is the fractional amount of O_2 in the matrix, P_{Ar} is the fractional amount of Ar in the matrix, and $^{12}C_n = 12!/(n!(12-n)!)$ is the number of combinations in which *n* O_2 molecules can be arranged around a single water molecule in an argon lattice. P_{oxy} and P_{Ar} are simply calculated from the ratios of the gaseous mixtures from which the matrixes are deposited.

As is shown in Figure 2, the amount of complex in the matrix is small compared with that of water monomer at low O_2 concentrations. Therefore, absorptions from the complex are also likely to be small in comparison with the dominating water vibrations. However, it can also be seen that as the O_2 concentration is increased, the amount of complex increases. To assign vibrations from the $H_2O{\cdot}O_2$ complex, we thus chose to vary the O_2 concentration while keeping the much lower H_2O concentration constant. Absorption bands that originate from $H_2O{\cdot}O_2$ should increase in intensity with increasing O_2 concentration.

This paper is concerned with the symmetric OH stretch (ν_1), HOH bend (ν_2), asymmetric OH stretch (ν_3), and OO stretch (ν_4) of the complex, and each vibration will be dealt with in turn. Table 3 lists the water monomer and water dimer vibrations that are the source of many of the absorptions in the spectra. The water monomer rotates in argon matrixes[30] and subsequently produces several rovibrational bands for each mode of vibration. However, a non-rotating monomer (nrm) of water is also found[30] in argon occurring near the rovibrational band center. It is thought that the rotation is hindered by inhomogeneity of the matrix or weak interactions with non-nearest neighbors.[40]

It is important to distinguish between absorptions due to vibrations from nrm and $H_2O{\cdot}O_2$. The disruption of the Ar lattice by O_2 may cause an increase in the nrm population. This means that a nrm absorption band would increase with increasing O_2 concentration. To discriminate between the absorptions of nrm and $H_2O{\cdot}O_2$, we have also measured the spectra of Ar matrixes containing *only* H_2O. Perchard[30] has identified bands at 1589.2, 3638.3, and 3736.0 cm^{-1} that exhibit an increase in intensity with increasing concentration and a decrease in intensity with increasing temperature. These bands are close to the rovibrational band centers and were assigned to nrm. We observe these bands at 1590.2, 3638.3 and 3736.2 cm^{-1}.

In Figure 3, we show the OH-stretching regions of both $H_2O{\cdot}O_2$ and nrm. The intensity of one peak in each of the ν_1 and ν_3 regions is observed to increase with increasing O_2 concentration. Similarly, in Figure 4, we give an overview spectrum of the HOH-bending and OO-stretching regions.

As is shown in Figure 5a−c, a reasonably broad absorption at 3731.6 cm^{-1} increases in intensity with increasing O_2 concentration in 1:*X*:1000 $H_2O/O_2/Ar$ matrixes. Fortunately, this absorption occurs in a "window" between the strong water monomer rovibrational absorption. However, the increase of O_2 concentration causes the rovibrational absorptions to broaden and decrease in intensity until they are almost fully quenched at a ratio of 1:150:1000 $H_2O/O_2/Ar$ in Figure 5c. From the probability distribution shown in Figure 2, it is unlikely that all the water molecules are complexed to an oxygen molecule, but it is more likely that oxygen doped into the argon lattice is sufficient to hinder the rotation of water. This is in agreement with previous studies.[41,42]

TABLE 3: Summary of H_2O Monomer and Dimer Vibrational Energies in Argon Matrixes as Reported in Ref 30

	ν_3/cm^{-1}	ν_1/cm^{-1}	ν_2/cm^{-1}
	H_2O Monomer		
rovibrational bands[a]	3711.3, 3724.9 3739.0, 3756.6	3606.8, 3622.7 3653.5, 3669.7	1573.1, 1607.9 1623.9, 1636.5
nrm	3736.0	3638.3	1589.2
	H_2O Dimer		
proton acceptor	3715.7, 3737.8	3633.1	1593.1
proton donor	3708.0	3574.0	1610.6

[a] For assignments to rovibrational states, refer to ref 29.

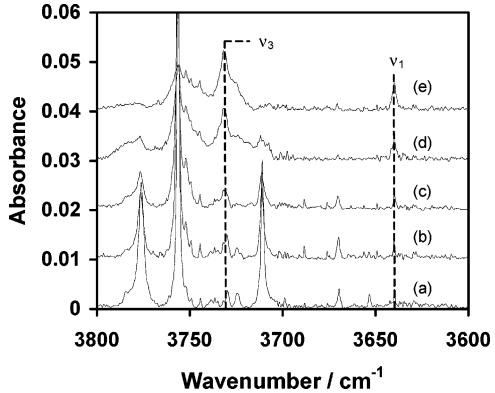

Figure 3. Infrared spectra in the OH-stretching region of (a) 1:0:1000 $H_2O/O_2/Ar$, (b) 1:10:1000 $H_2O/O_2/Ar$, (c) 1:50:1000 $H_2O/O_2/Ar$, (d) 1:100:1000 $H_2O/O_2/Ar$, and (e) 1:150:1000 $H_2O/O_2/Ar$ matrixes at 11.5 K.

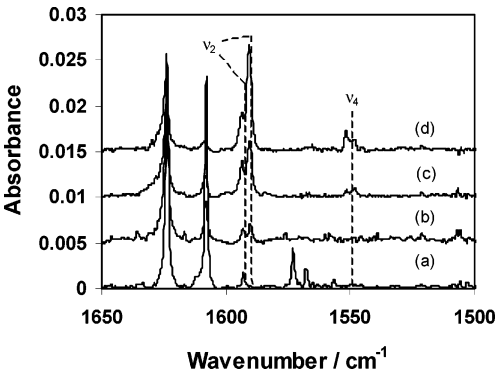

Figure 4. Infrared spectra in the HOH-bending and OO-stretching region of (a) 1:0:3000 $H_2O/O_2/Ar$, (b) 1:100:3000 $H_2O/O_2/Ar$, (c) 1:200:3000 $H_2O/O_2/Ar$, and (d) 1:300:3000 $H_2O/O_2/Ar$ matrixes at 11.5 K.

On the basis of our calculations, we predict a 2 cm^{-1} red shift of the ν_3 vibration of H_2O upon complexation to O_2. This is in good agreement with the difference between the ν_3 vibrational frequency of nrm observed at 3736.2 cm^{-1} and the 3731.6 cm^{-1} absorption. In Figure 3, a weak, partially obscured shoulder at ~3736 cm^{-1}, that broadens the main 3731.6 cm^{-1} absorption, is present at high O_2 concentrations. The intensity of the ν_3 vibration of nrm at an H_2O/Ar ratio of 1:1000 is very weak, so only a small absorption from nrm is to be expected. At more dilute concentrations of 1:*X*:3000 $H_2O/O_2/Ar$ (Figure 5d,e), we would not expect to observe any absorption from nrm. This is confirmed with only the 3731.6 cm^{-1} band present at this low water concentration, indicating that the water concentration is too low to detect nrm, even with O_2 in the matrix. We thus assign the 3731.6 cm^{-1} band to the ν_3 vibration of the $H_2O \cdot O_2$ complex.

The ν_1 vibration of water monomer is considerably less intense than that of the ν_3 mode in agreement with our calculations shown in Table 1. The spectra (Figure 6) exhibit rovibrational absorptions that are quenched as the water molecule's rotation is hindered by the inhomogeneity of the argon matrix. An absorption at 3640.0 cm^{-1} is observed to increase with increasing oxygen concentration in 1:*X*:1000 $H_2O/O_2/Ar$ matrixes, as shown in Figure 6a−c. We tentatively assign this transition to the ν_1 vibration of the $H_2O \cdot O_2$ complex. This lies very close to the nrm vibrational frequency of 3638.3 cm^{-1}. This observed shift is in good agreement with our calculated blue shift of 3 cm^{-1} of the symmetric OH stretch of $H_2O \cdot O_2$ compared with monomeric H_2O. The observed frequency shifts from monomer in the $H_2O \cdot O_2$ and $H_2O \cdot N_2$ complexes are small, as expected from the weak interaction.[23] The frequency shifts are slightly larger in the $H_2O \cdot N_2$ complex, as might be expected from the relative binding energies.

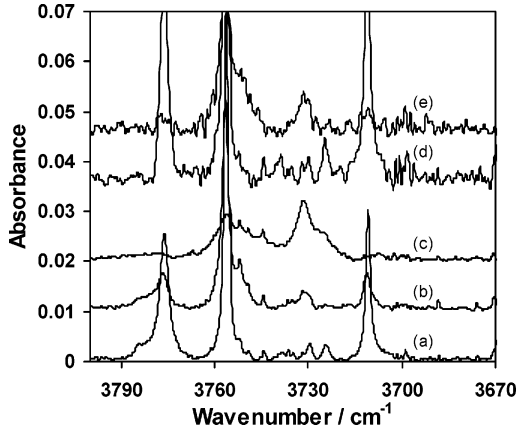

Figure 5. Infrared spectra in the OH-stretching region of (a) 1:0:1000 $H_2O/O_2/Ar$, (b) 1:50:1000 $H_2O/O_2/Ar$, (c) 1:150:1000 $H_2O/O_2/Ar$, (d) 1:0:3000 $H_2O/O_2/Ar$ (×5), and (e) 1:300:3000 $H_2O/O_2/Ar$ (×5) matrixes at 11.5 K.

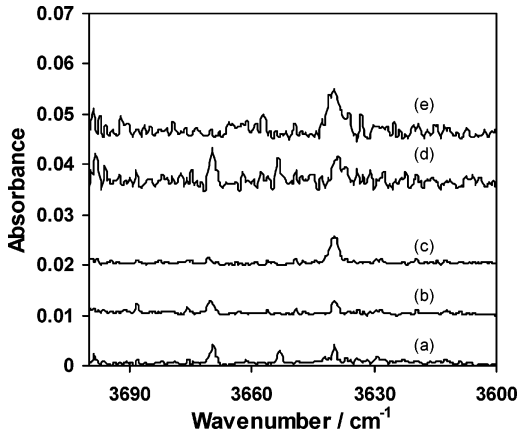

Figure 6. Infrared spectra in the OH-stretching region of (a) 1:0:1000 $H_2O/O_2/Ar$, (b) 1:50:1000 $H_2O/O_2/Ar$, (c) 1:150:1000 $H_2O/O_2/Ar$, (d) 1:0:3000 $H_2O/O_2/Ar$ (×5), and (e) 1:300:3000 $H_2O/O_2/Ar$ (×5) matrixes at 11.5 K.

In Table 4, we have given the observed and calculated transitions for water and the $H_2O \cdot O_2$ complex. We notice that the ν_3 vibrations are red shifted and the ν_1 transitions blue shifted

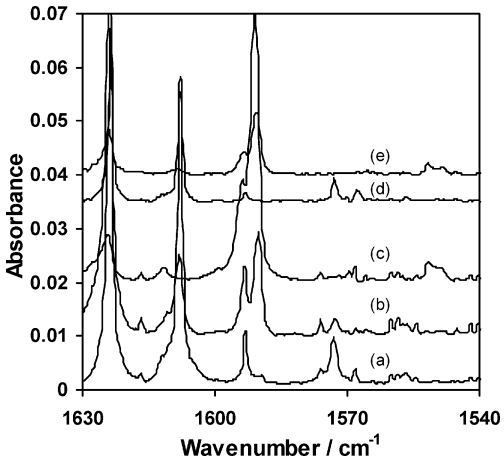

Figure 7. Infrared spectra in the HOH-bending region of (a) 1:0:1000 $H_2O/O_2/Ar$, (b) 1:50:1000 $H_2O/O_2/Ar$, (c) 1:150:1000 $H_2O/O_2/Ar$, (d) 1:0:3000 $H_2O/O_2/Ar$, and (e) 1:300:3000 $H_2O/O_2/Ar$ matrixes at 11.5 K.

TABLE 4: Comparison of the Calculated and Experimentally Determined Vibrational Energies of H_2O and $H_2O{\cdot}O_2$

	calcd H_2O	calcd $H_2O{\cdot}O_2$	exptl H_2O	exptl $H_2O{\cdot}O_2$
mode	energy/cm^{-1}	energy/cm^{-1}	energy/cm^{-1}	energy/cm^{-1}
ν_4		1551		1551
ν_2	1596	1593	1590	1590
ν_1	3658	3661	3638	3640
ν_3	3755	3753	3736	3731

upon complexation in agreement with our calculations. Our calculations predict that the intensity (Table 1) of the ν_1 vibration of $H_2O{\cdot}O_2$ is about 15 times less than that for the ν_3 vibration. Experimentally, this ratio is hard to determine accurately because of the overlapping broad bands of the ν_3 vibration, but we estimate the ν_1 band to be about 5 times less intense than the ν_3 band.

Figure 6 shows that an absorption band at 3640 cm^{-1} is observed, even without the presence of O_2 in the matrix. This absorption has not been assigned in previous investigations of matrix isolated water,[30,43,44] although it appears to originate from water, as the intensity is dependent upon water concentration. However, when we keep the H_2O concentration fixed, we still find a dependence upon O_2 concentration. This observation, in addition to the excellent agreement with the frequency shift of our calculations, is further evidence for the assignment of the 3640.0 cm^{-1} band to the ν_1 vibration of the $H_2O{\cdot}O_2$ complex. We do acknowledge however that there is a contribution from a species other than $H_2O{\cdot}O_2$.

The water monomer's ν_2 bending mode of vibration in an argon matrix is also split into a number of rovibrational lines. Upon increasing the O_2 concentration in the matrix, the rovibrational lines are quenched as described above. Two absorption lines at 1590.2 and 1593.6 cm^{-1} are observed to increase with increasing O_2 concentration (Figure 7). The absorption at 1590.2 cm^{-1} shows the strongest concentration dependence and has a similar frequency to the ν_2 mode of the nrm (Table 3).

The band at 1593.6 cm^{-1} is close to the observed frequency of the ν_2 proton acceptor mode of the water dimer.[30] However, the water dimer is not expected to show any dependence upon O_2 concentration in the matrix and the lack of water dimer transitions in other regions of the spectrum does not support an assignment of this band to the water dimer. We clearly observe

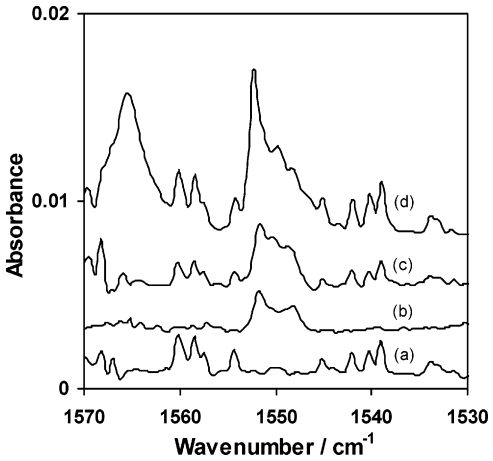

Figure 8. Infrared spectra in the OO-stretching region of (a) 100:1000 O_2/Ar, (b) 1:300:3000 $H_2O/O_2/Ar$, (c) 1:150:1000 $H_2O/O_2/Ar$, and (d) 1:500 H_2O/O_2 matrixes at 11.5 K.

nrm in the water-only matrixes at 1590.2 cm^{-1}, so we do not believe the 1593.6 cm^{-1} band is nrm.

We assign the 1590.2 cm^{-1} band to the ν_2 vibration of $H_2O{\cdot}O_2$ on the basis of its O_2 concentration dependence. We also tentatively assign the 1593.6 cm^{-1} band to the ν_2 vibration of $H_2O{\cdot}O_2$. While the band at 1590.2 cm^{-1} has the same frequency as the nrm vibration, the 1:*X*:3000 spectra in Figure 7d,e indicate that the absorption at these low concentrations cannot be due to nrm. In addition, Coussan et al.[23] do not observe nrm at these concentrations in their $H_2O/N_2/Ar$ matrixes. Simply, the intensity of the 1590.2 cm^{-1} band is too large to come from nrm.

The infrared (IR) forbidden stretching vibration (ν_4) of O_2 becomes slightly IR active in the $H_2O{\cdot}O_2$ complex. We calculate this OO-stretching transition to be red shifted by 5 cm^{-1} in the complex compared to that in molecular O_2. The OO stretch in molecular oxygen has previously been observed when other molecules act to lower the symmetry of O_2.[43] It has also been observed in solid O_2 but is due to defects in the O_2 lattice.[44] In each case, the O_2 fundamental is observed at ~1551 cm^{-1}. Figure 7 shows the growth of an absorption band at 1551.9 cm^{-1} with increasing O_2 concentration. At low water concentrations, the vibration is observed as a doublet, with a second peak at 1548.8 cm^{-1}. At higher water concentrations, a third peak at 1550.5 cm^{-1} is also present (Figure 8). No absorption peaks are observed when water is absent, indicating that the peaks are induced by water.

At first, it is attractive to assign the higher energy peak to a non-complexed O_2 molecule in a non-homogeneous site and the lower energy peak to the $H_2O{\cdot}O_2$ complex. The magnitude and direction of the shift would agree with our calculations. However, a similar doublet is observed by Xie et al.[45] in glassy Ar/O_2 mixed crystals in which magnetic and quadrupolar moments induce local ordering and cause splitting of the vibration. In addition, they found that the two bands are dependent upon the O_2/Ar ratio. The higher energy band dominated as their O_2 concentration approached the much lower O_2 concentration used in the present experiments. The lowest O_2/Ar ratio these workers used was 4.2:10 O_2/Ar, whereas our ratios were typically 0.5−1.5:10 O_2/Ar. Nevertheless, in our spectra, the high energy band is the most intense in agreement with Xie et al.[45]

If the bands observed around 1550 cm^{-1} are due to O_2−Ar interactions, then it is most likely that the absorptions are from noncomplexed O_2 molecules in several nonhomogeneous sites and that the low intensity 5 cm^{-1} red-shift peak, predicted from

theory, is too weak to be observed. However, in the light of an additional experiment, we believe this may not be the case. We measured the spectrum of a 1:500 H_2O/O_2 sample at 11 K, that is, water in an oxygen matrix. We found that the same absorption structure observed in Ar matrixes was present (Figure 8). The absence of Ar means the absorption band structure cannot be from O_2-Ar interactions. A report of the OO vibration from O_2 produced in UV-irradiated H_2O ice[43] at 1550 cm^{-1} unfortunately does not show spectra which would allow a further comparison, but once again, the frequency is in agreement with our present data.

We believe the agreement in observations between H_2O/O_2 in Ar matrixes, H_2O in O_2 matrixes, and O_2 in H_2O matrixes indicates that H_2O must be interacting in our matrix isolation experiments in very close proximity to O_2 in order to induce the OO-stretching vibration. The band structure is not due to magnetic and quadrupolar interactions with Ar but must be due to interactions with a water molecule. There still lies the possibility that the structure of the O_2 absorption band is due to nearest neighbor (complexed) and non-nearest neighbor interactions of O_2 and H_2O, but the agreement between the Ar matrix and O_2 matrix experiments might not be expected to correlate so well if this was the case. Other experimental techniques such as molecular beam investigations might help to solve this issue.

Conclusions

We have provided evidence for the existence of the $H_2O \cdot O_2$ complex in an argon matrix. Although the binding energy of the complex is very weak, we calculate small, but measurable differences in its infrared spectrum compared with the individual monomer units. On the basis of these shifts and the relative intensities of the bands, absorption features in IR spectra of $H_2O/O_2/Ar$ matrixes have been assigned to vibrations of the $H_2O \cdot O_2$ complex. This identification of the complex may possibly help astronomers identify O_2 in icy satellite surfaces and interstellar grains.

Acknowledgment. We thank Mr. N. Hamilton, Chemistry Workshop, UWA; Professor R. E. Johnson, University of Virginia; and Professor J. P. Perchard, Université Pierre et Marie Curie. The following sources of funds are gratefully acknowledged: the Australian Government for a postgraduate scholarship for P.D.C.; The Foundation for Research, Science and Technology for Bright Future Scholarships for D.P.S. and T.W.R.; and The University of Western Australia and The Marsden Fund administrated by the Royal Society of New Zealand for financial support.

References and Notes

(1) Heidt, L. J.; Ekstrom, L. *J. Am. Chem. Soc.* **1957**, *79*, 1260−1261.
(2) Heidt, L. J.; Johnson, A. M. *J. Am. Chem. Soc.* **1957**, *79*, 5587−5593.
(3) Byers Brown, W. *Chem. Phys. Lett.* **1995**, *235*, 94−98.
(4) Byers Brown, W.; Hillier, I. H.; Masters, A. J.; Palmer, I. J.; Dos Santos, D. H. V.; Stein. M.; Vincent, M. A. *Faraday Discuss.* **1995**, *100*, 253−267.
(5) Dos Santos, D. H. V.; Vaughn, S. J.; Akhmatskaya, E. V.; Vincent, M. A.; Masters, A. J. *J Chem. Soc., Faraday Trans.* **1997**, *93*, 2781−2785.
(6) Cacace, F.; De Petris, G.; Pepi, F.; Troiani, Anna. *Angew. Chem., Int. Ed.* **2000**, *39*, 367−369.
(7) Byers Brown, W.; Vincent, M. A.; Trollope, K.; Hillier, I. H. *Chem. Phys. Lett.* **1992**, *192*, 213−216.
(8) Vincent, M. A.; Hillier, I. H. *J. Phys. Chem.* **1995**, *99*, 3109−3133.
(9) Palmer, I. J.; Byers Brown, W.; Hillier, I. H. *J. Chem. Phys.* **1996**, *104*, 3198−3204.
(10) Svishchev, I. M.; Boyd, R. J. *J. Phys. Chem. A* **1998**, *102*, 7294−7296.
(11) Kjaergaard, H. G.; Low, G. R.; Robinson, T. W.; Howard, D. L. *J. Phys. Chem. A.* **2002**, *106*, 8955−8962.
(12) Robinson, T. W.; Kjaergaard, H. G. *J. Chem. Phys.* **2003**, *119*, 3717−3720.
(13) Kasai, Y.; Sumiyoshi, Y.; Endo, Y. 55th International Symposium on Molecular Spectroscopy, The Ohio State University, Columbus, OH, 2000.
(14) Wayne, R. P. *Chemistry of Atmospheres*, 2nd ed.; Clarendon Press: Oxford, U.K., 1991.
(15) Vaida, V.; Headrick, J. E. *J. Phys. Chem. A* **2000**, *104*, 5401−5412.
(16) Hansen, J. C.; Francisco, J. S. *ChemPhysChem* **2002**, *3*, 833−840.
(17) Kjaergaard, H. G.; Robinson, T. W.; Howard, D. L.; Daniel, J. S.; Headrick, J. E.; Vaida, V *J. Phys. Chem. A* **2003**, *107*, 10680−10686.
(18) Daniel, J. S.; Solomon, S.; Kjaergaard, H. G.; Schofield, D. P. *Geophys. Res. Lett.* **2004**, *31*, L06118.
(19) Spencer, J. R.; Calvin, W. M.; Person, M. J. *J. Geophys. Res.* **1995**, *100*, 19049−19056.
(20) Spencer, J. R.; Calvin, W. M. *Astron. J.* **2002**, *124*, 3400−3403.
(21) Calvin, W. M.; Johnson, R. E.; Spencer, J. R. *Geophys. Res. Lett*. **1996**, *23*, 673−676.
(22) Cooper, P. D.; Johnson, R. E.; Quickenden, T. I. *Planet. Space. Sci.* **2003**, *51*, 183−192.
(23) Coussan, S.; Loutellier, A.; Perchard, J. P.; Racine, S.; Bouteiller, Y. *J. Mol. Struct.* **1998**, *471*, 37−47.
(24) Langford, V. S.; McKinley, A. J.; Quickenden, T. I. *J. Am. Chem. Soc.* **2000**, *122*, 12859−12863.
(25) Cooper, P. D.; Kjaergaard, H. G.; Langford, V. S.; McKinley, A. J.; Quickenden, T. I.; Schofield, D. P. *J. Am. Chem. Soc.* **2003**, *125*, 6048−6049.
(26) Engdahl, A.; Karlström, G.; Nelander, B. *J. Chem. Phys.* **2003**, *118*, 7797−7802.
(27) Schriver, L.; Barreau, C.; Schriver, A. *Chem. Phys.* **1990**, *140*, 429−438.
(28) Zhou, M.; Zeng, A.; Wang, Y.; Kong, Q.; Wang, Z.-X.; van Ragué Schleyer, P. *J. Am. Chem. Soc.* **2003**, *125*, 11512−11513.
(29) Nelander, B. *J. Phys. Chem. A* **1997**, *101*, 9092−9096.
(30) Perchard, J. P. *Chem. Phys.* **2001**, *273*, 217−233.
(31) Atkins, P. W.; Friedman, R. S. *Molecular Quantum Mechanics*, 3rd ed.; Oxford University Press: Oxford, U.K., 1997.
(32) Kjaergaard, H. G.; Henry, B. R.; Wei, H.; Lefebvre, S.; Carrington, T., Jr.; Mortensen, O. S.; Sage, M. L. *J. Chem. Phys*. **1994**, *100*, 6228−6239.
(33) Schofield, D. P.; Kjaergaard, H. G. *Phys. Chem. Chem. Phys*. **2003**, *5*, 3100−3105.
(34) Halonen, L.; Carrington, T., Jr. *J. Chem. Phys.* **1988**, *88*, 4171−4185.
(35) Sowa, M. G.; Henry, B. R.; Mizugai, Y. *J. Phys. Chem.* **1991**, *95*, 7659−7664.
(36) Low, G. R.; Kjaergaard, H. G. *J. Chem. Phys*. **1999**, *110*, 9104−9115.
(37) Krupenie, P. *J. Phys. Chem. Ref. Data* **1972**, *1*, 423−534.
(38) Frisch, M. J.; Trucks, G. W.; Schlegel, H. B.; Gill, P. M. W.; Johnson, B. G.; Robb, M. A.; Cheeseman, J. R.; Keith, T.; Petersoon, G. A.; Montgomery, J. A.; Raghavachari, K.; Al-Laham, M. A.; Zakrzewski, V. G.; Ortiz, J. V.; Foresman, J. B.; Cioslowski, J.; Stefanov, B. B.; Nanyakkara, A.; Challacombe, M.; Peng, C. Y.; Ayala, P. Y.; Chen, W.; Wong, M. W.; Andres, J. L.; Replogle, E. S.; Gomperts, R.; Martin, R. L.; Fox, D. J.; Binkley, J. S.; Defrees, D. J.; Baker, J.; Stewart, J. P.; Head-Gordon, M.;, Gonzalez, C.; Pople, J. A. *Gaussian 94*, revision d.4; 1995.
(39) Sabu, A.; Kondo, S.; Miura, N.; Hashimoto, K. *Chem. Phys. Lett.* **2004**, *391*, 101−105.
(40) Engdahl, A.; Nelander, B. *J. Mol. Struct.* **1989**, *193*, 101−109.
(41) Bentwood, R. M.; Barnes, A. J.; Orville-Thomas, W. J. *J. Mol. Spectrosc.* **1980**, *54*, 391−404.
(42) Ayers, G. P.; Pullin, A. D. E. *Spectrochim. Acta* **1976**, *32A*, 1629−1639.
(43) Gerakines, P. A.; Schutte, W. A.; Ehrenfreund, P. *Astron. Astrophys*. **1996**, *312*, 289−305.
(44) Cairns, B. R.; Pimentel, G. C. *J. Chem. Phys.* **1965**, *43*, 3432−3438.
(45) Xie, J.; Enderle, M.; Knorr, K.; Jodl, H. *Phys Rev. B* **1997**, *55*, 8194−8200.